Immune Netw. 2022 Oct;22(5):e43
https://doi.org/10.4110/in.2022.22.e43
pISSN 1598-2629·eISSN 2092-6685

IMMUNE NETWORK

Brief Communication

Check for updates

1,3-Dibenzyl-5-Fluorouracil Prevents Ovariectomy-Induced Bone Loss by Suppressing Osteoclast Differentiation

Hyoeun Jeon [1,†], **Jungeun Yu** [1,†], **Jung Me Hwang** [2], **Hye-Won Park** [1], **Jiyeon Yu** [1], **Zee-Won Lee** [3], **Taesoo Kim** [4], **Jaerang Rho** [1,*]

[1]Department of Microbiology and Molecular Biology, Chungnam National University, Daejeon 34134, Korea
[2]Center for Genomic Integrity, Institute for Basic Science, Ulsan 44919, Korea
[3]bHLBIO, Cheongju 28119, Korea
[4]Herbal Medicine Research Division, Korea Institute of Oriental Medicine, Daejeon 34054, Korea

OPEN ACCESS

Received: Mar 15, 2022
Revised: Jul 11, 2022
Accepted: Jul 27, 2022
Published online: Sep 26, 2022

***Correspondence to**
Jaerang Rho
Department of Microbiology and Molecular Biology, Chungnam National University, 99 Daehak-ro, Yuseong-gu, Daejeon 34134, Korea.
Email: jrrho@cnu.ac.kr

[†]Hyoeun Jeon and Jungeun Yu contributed equally to this work.

ORCID iDs
Hyoeun Jeon
https://orcid.org/0000-0002-2141-6123
Jungeun Yu
https://orcid.org/0000-0002-4036-4867
Jung Me Hwang
https://orcid.org/0000-0001-7246-4646
Hye-Won Park
https://orcid.org/0000-0002-0566-0636
Jiyeon Yu
https://orcid.org/0000-0001-5368-3093
Zee-Won Lee
https://orcid.org/0000-0001-7338-4461

ABSTRACT

Osteoclasts (OCs) are clinically important cells that resorb bone matrix. Accelerated bone destruction by OCs is closely linked to the development of metabolic bone diseases. In this study, we screened novel chemical inhibitors targeting OC differentiation to identify drug candidates for metabolic bone diseases. We identified that 1,3-dibenzyl-5-fluorouracil, also named OCI-101, is a novel inhibitor of osteoclastogenesis. The formation of multinucleated OCs is reduced by treatment with OCI-101 in a dose-dependent manner. OCI-101 inhibited the expression of OC markers via downregulation of receptor activator of NF-κB ligand and M-CSF signaling pathways. Finally, we showed that OCI-101 prevents ovariectomy-induced bone loss by suppressing OC differentiation in mice. Hence, these results demonstrated that OCI-101 is a good drug candidate for treating metabolic bone diseases.

Keywords: Osteoclasts; Osteoclastogenesis; 1,3-Dibenzyl-5-fluorouracil; Ovariectomy; Osteoporosis

INTRODUCTION

Bone is continuously maintained by the process of bone remodeling through the balanced actions of bone-resorbing osteoclasts (OCs) and bone-forming osteoblasts (1-3). OCs, the only cells with bone-resorbing activity, play clinically important roles in metabolic bone diseases, such as postmenopausal osteoporosis and osteoarthritis, which are characterized by accelerated bone destruction by OCs (2,4). Therefore, inhibition of excessive OC bone-resorbing activity and OC differentiation play a key role in the treatment of metabolic bone diseases (2,3).

Mature bone-resorbing OCs are multinucleated giant cells derived from cell fusion of monocyte/macrophage lineage precursors by a process of cellular differentiation called OC differentiation or osteoclastogenesis (2,3). Osteoclastogenesis is mainly regulated by 2 cytokines, M-CSF and RANK ligand (RANKL), which are produced by osteoblasts and activated immune cells (2,3). RANK-RANKL signaling is a key process in OC differentiation

Taesoo Kim
https://orcid.org/0000-0001-7503-9725
Jaerang Rho
https://orcid.org/0000-0002-0019-4939

Conflict of Interest
The authors declare no potential conflicts of interest.

Abbreviations
BMD, bone mineral density; BMM, bone marrow macrophage; BMOC, bone marrow-derived osteoclast; IKK, inhibitor of κB kinase; KCB, Korea Chemical Bank; micro-CT, micro-computed tomography; OC, osteoclast; OVX, ovariectomy; RANKL, receptor activator of NF-κB ligand; TRAF, tumor necrosis factor receptor-associated factor; TRAP, tartrate-resistant acid phosphatase.

Author Contributions
Conceptualization: Yu J,[1] Jeon H, Hwang JM; Data curation: Yu J,[1] Jeon H, Hwang JM, Kim T; Formal analysis: Lee ZW, Rho J; Funding acquisition: Rho J; Investigation: Yu J,[1] Jeon H, Hwang JM; Methodology: Park HW, Yu J,[2] Kim T; Project administration: Rho J, Lee ZW; Resources: Lee ZW; Supervision: Rho J; Writing - original draft: Jeon H, Yu J[1]; Writing - review & editing: Rho J.
Yu J,[1] Jungeun Yu; Yu J,[2] Jiyeon Yu.

and bone-resorbing function. Upon RANKL stimulation, RANK recruits tumor necrosis factor receptor-associated factors (TRAFs) to activate downstream signaling cascades of adaptors/kinases, such as IκB kinases (IKKs), Vav3, c-Src and MAPKs, including p38, JNK and ERK (3,5). M-CSF also activates p38, JNK, ERK and Akt signaling that regulate OC proliferation and survival (2,3). The final consequence of RANKL and M-CSF signaling cascades is the activation of osteoclastogenic transcription factors, such as NF-κB, AP-1, cAMP-response element-binding protein and NFATc1, which induce the expression of OC markers, such as tartrate-resistant acid phosphatase (TRAP), OC-associated receptor, dendritic cell-specific transmembrane protein, B-lymphocyte induced maturation protein 1 and cathepsin K (3,6-8).

Osteoporosis is most common in postmenopausal women (9). Estrogen has a protective effect on bones by inhibiting bone loss (10). In postmenopausal osteoporotic patients, estrogen deficiency can lead to excessive bone resorption due to increases in both OC differentiation and OC activity, which causes rapid bone loss (9). Thus, estrogen or estrogen signal-related therapies targeting OC differentiation/activity, including estrogen replacement and selective estrogen receptor modulators, have been regarded as treatments for postmenopausal osteoporosis (11). In long-term therapy, however, these therapeutic options are limited by adverse effects, including an increased risk of uterine or breast cancer and cardiovascular events (9,12). Bisphosphonates (a classic anti-resorptive agent) and denosumab (a human monoclonal antibody to RANKL) are currently the most widely used therapies for the treatment of postmenopausal osteoporosis (13). Bisphosphonates, such as alendronate, risedronate and zoledronate, are considered the first-line treatment for postmenopausal osteoporosis (13,14). Bisphosphonates bind to calcium in bone and inhibit bone resorption by reducing OC activity or by inducing OC apoptosis, leading to reduced fracture risk (14-16). Denosumab blocks the RANK-RANKL interaction, thereby inhibiting both OC differentiation and OC activity and enhancing bone strength (17). Denosumab is also considered both a first-line agent and an alternative to bisphosphonates in the treatment of postmenopausal osteoporosis (18). In long-term therapy, bisphosphonate treatment results in a plateau in bone mineral density (BMD) response after 3–5 years, while denosumab treatment leads to continuously increasing BMD for up to 10 years of treatment (19-21). Denosumab treatment increases BMD and reduces cortical porosity at all measured skeletal sites and decreases expression of biochemical markers of bone turnover (18,22). Therefore, denosumab administration targeting RANK-RANKL signaling can be considered the preferred choice for the treatment of postmenopausal osteoporosis (18). Both bisphosphonates and denosumab are generally considered to be safe, but prolonged medication is also associated with adverse effects, such as jaw osteonecrosis, hypocalcemia, gastrointestinal symptoms and atypical femoral fractures (18,23,24). Thus, it is necessary to find new and more effective drug candidates for the management of postmenopausal osteoporosis and inflammatory bone-related diseases.

In this study, we discovered a novel chemical inhibitor named OCI-101, 1,3-dibenzyl-5-fluorouracil, targeting OC differentiation. We demonstrate that OCI-101 acts as an inhibitor of osteoclastogenesis. The formation of multinucleated OCs is dose-dependently inhibited by OCI-101 treatment. Finally, we show that OCI-101 prevents ovariectomy (OVX)-induced bone loss by suppressing OC differentiation in mice.

IMMUNE NETWORK

MATERIALS AND METHODS

Reagents, antibodies and mice

1,3-Dibenzyl-5-fluorouracil was purchased from Santa Cruz Biotechnology (Santa Cruz, CA, USA). A chemical library with a total of 16,380 unique chemical compounds was obtained from the Korea Chemical Bank (KCB). Recombinant human soluble RANKL and human M-CSF were prepared as previously described (25,26). Antibodies were purchased from Cell Signaling Technology (Beverly, MA, USA). Mice were purchased from Daehan Biolink Co. (Umsung, Korea), and the animal study was approved (approval No. CNU-00326 and CNU-00114) by the Animal Experiment Ethics Committee of Chungnam National University.

OC differentiation, analysis and cytotoxicity assay

Osteoclastogenesis was performed as described previously (25,26). Briefly, bone marrow cells collected from the tibias and femurs of 6-week-old C57BL/6J male mice were cultured at 1×10^5 cells/well in 96-well plates in the presence of 50 ng/ml M-CSF and 200 ng/ml RANKL for 4 days. Bone marrow-derived OCs (BMOCs) were further analyzed by TRAP staining and solution assays. For the TRAP solution assay, BMOCs were fixed and incubated with the *p*-nitrophenyl phosphate substrate for 30 min. The supernatant was then mixed with 1 N NaOH, and TRAP activities were analyzed by measuring the absorbance at 405 nm in each well using a microplate reader (Bio–Rad, Hercules, CA, USA). For the TRAP staining assay, the cells were stained with naphthol AS phosphate and fast red violet for 20–30 min at room temperature. TRAP-positive multinucleated BMOCs ($TRAP^+$ MNCs) with more than 3 nuclei were considered multinucleated OCs. For the cytotoxicity assay, bone marrow cells (1×10^5 cells/well in 96-well plates) were differentiated into bone marrow-derived macrophages (BMMs) with 50 ng/ml M-CSF alone in the presence or absence of OCI-101 (25–100 μM) for 4 days. Real-time PCR analysis and pit formation assay were performed as previously described (27,28). The cytotoxicity of OCI-101 in BMMs was analyzed using the Cell Counting Kit-8 (Dojindo Lab., Kumamoto, Japan) according to the manufacturer's recommendations. The analyses of RANKL-induced signaling using immunoblotting were performed as described previously (25,26). BMMs were preincubated with 100 μM OCI-101 for 12 h before RANKL or M-CSF stimulation. To induce RANKL or M-CSF signaling, BMMs precultured for 2 h without RANKL or M-CSF. The cells were stimulated with RANKL (200 ng/ml) or M-CSF (50 ng/ml) for the indicated times, and the cell lysates were subjected to immunoblot analysis with antibodies.

Bone analysis by micro-computed tomography (micro-CT) and histological analysis

Bone analysis was performed as previously described (28,29). Briefly, C57BL/6J female mice (8-week-old, n=10–11 per group) were randomly divided into 4 groups: sham operation (Sham), OVX with a vehicle, ovariectomy with a low dose of OCI-101 (OVX + OCI-101 [1 mg/kg]) and ovariectomy with a high dose of OCI-101 (OVX + OCI-101 [10 mg/kg]). OVX was performed by surgical removal of ovaries, and sham surgery was performed by identifying both ovaries. A week after surgery, the mice were injected intraperitoneally with OCI-101 (1–10 mg/kg) or vehicle each day for 3 wk. For micro-CT analysis, femurs were fixed with 10% formalin, and trabecular morphometry of distal femurs was performed using micro-CT (SkyScan 1076, Bruker micro-CT; Bruker, Kontich, Belgium). For histological analysis, the femurs were decalcified in 15% EDTA solution at 4°C for 3 wk and embedded in paraffin. Paraffin sections were stained with TRAP and hematoxylin, and the $TRAP^+$ OCs were counted by visualization under a microscope.

https://doi.org/10.4110/in.2022.22.e43

Statistical analysis.

The data represent the mean ± SD (at least n=3 per group). Statistical analyses were performed using 2-tailed Student's t-test or 1- or 2-way ANOVA. The p-values <0.05 were considered statistically significant.

RESULTS

OCI-101 inhibits OC differentiation

Inhibitors of osteoclastogenesis were screened by OC differentiation assays using a KCB chemical library containing a total of 16,380 unique chemical compounds at a chemical concentration of 5 μM. We identified several inhibitory candidates, named the OCI series (data not shown). Among them, we discovered a novel chemical inhibitor named OCI-101, or 1,3-dibenzyl-5-fluorouracil, that targeted OC differentiation (**Fig. 1A**). First, we examined the cytotoxicity of OCI-101 by a cell proliferation assay with BMMs. BMMs were stimulated for 4 days with M-CSF alone (50 ng/ml) in the presence of OCI-101 compounds (0–100 μM). We did not observe OCI-101 cytotoxicity at any of the tested concentrations in BMMs after 4 days of culture (**Fig. 1B**). To test the inhibitory effect of OCI-101 on OC differentiation, BMMs were differentiated into BMOCs by stimulation with M-CSF (50 ng/ml) and RANKL (200 ng/ml) in the presence or absence of OCI-101. After 4 days of culture, the cells were fixed, and the fixed cells were analyzed by TRAP solution assay and TRAP staining to determine the number of differentiated multinucleated OCs ($TRAP^+$ MNC). OCI-101-treated BMMs showed a marked dose-dependent reduction in the differentiation of multinucleated OCs when compared to that of the mock-treated control (**Fig. 1C**). Furthermore, the number of $TRAP^+$ MNCs and TRAP activity were dose-dependently decreased by OCI-101 treatment (**Fig. 1D**). Similarly, the resorption area was reduced significantly by OCI-101 (**Fig. 1E**). Consistent with these results, we observed that the expression of OC markers was inhibited by OCI-101 (**Fig. 1F**). These results suggest that OCI-101 is an inhibitor targeting OC differentiation.

OCI-101 inhibits RANKL and M-CSF signaling pathway

We next analyzed the effect of OCI-101 on the RANKL- and M-CSF-induced signaling pathway. To induce RANKL signaling, BMMs precultured for 2 h without RANKL treatment were stimulated with 200 ng/ml RANKL at the indicated times. We then examined the activation of NF-κB and MAPKs by RANKL stimulation in OCI-101-treated BMMs. Upon RANKL stimulation, the phosphorylation of IκBα, p65 and ERK was inhibited by OCI-101 treatment, but not JNK phosphorylation, compared to the mock-treated control. In contrast, the phosphorylation of p38 was slightly enhanced by OCI-101 treatment (**Fig. 2A**). Furthermore, we observed that the phosphorylation of JNK, Akt and ERK following M-CSF stimulation was inhibited by OCI-101 treatment, but not IκBα, p65 and p38 phosphorylation (**Fig. 2B**). These results indicate that OCI-101 negatively regulates osteoclastogenesis via modulating multiple RANKL- and M-CSF-induced signaling pathways.

OCI-101 inhibits OVX-induced OC formation in mice

To examine the effects of OCI-101 on OC formation *in vivo*, C57BL/6 female mice were subjected to OVX or sham surgery. OVX mice were injected intraperitoneally with OCI-101 or vehicle each day for 3 wk. The femurs were collected, fixed and analyzed by TRAP staining and hematoxylin counterstaining. Finally, we compared bone histological morphology and OC formation in the trabecular region of femurs. OVX mice showed significantly reduced trabecular bones compared to those of sham control mice (**Fig. 3A**). After treatment with OCI-101 in OVX mice,

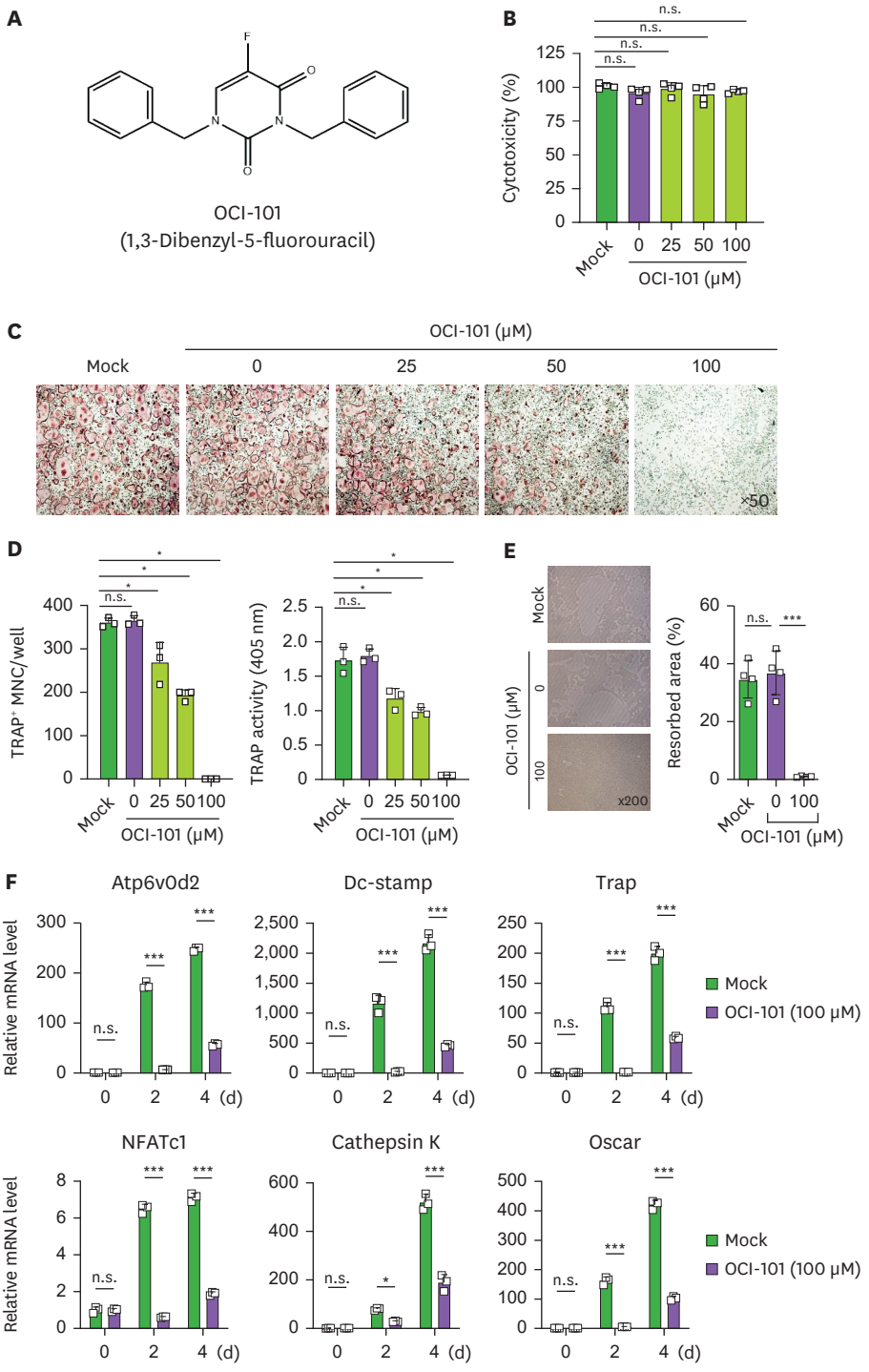

Figure 1. OCI-101 inhibits OC differentiation. (A) Chemical structures of OCI-101. (B) Cytotoxicity tests for OCI-101 in BMMs. Bone marrow cells were cultured with the indicated doses of OCI-101 in the presence of M-CSF (50 ng/ml) for 4 days. Cytotoxicity was measured by a Cell Counting Kit-8 assay kit. (C) The inhibition of BMOC differentiation by OCI-101. BMOCs were differentiated with the indicated doses of OCI-101 in the presence of M-CSF (50 ng/ml) and RANKL (200 ng/ml) for 4 days. BMOCs were analyzed by TRAP staining and photographed (original magnification, ×50). (D) Summary of the inhibitory effects of OCI-101 in the BMOC formation assay. The number of TRAP⁺ MNCs (≥3 nuclei) was counted (left panel). TRAP solution assays were performed (right panel). (E) The inhibition of resorption pit formation by OCI-101. Resorption pits were visualized (left panel, original magnification, ×200) and analyzed by using Image J software (right panel). (F) The inhibition of OC marker expression by OCI-101. Total RNA was prepared from BMOCs and subjected to real-time PCR analysis for OC marker expression. The data were normalized to β-actin.
n.s., not significant.
*p<0.05; ***p<0.001.

https://doi.org/10.4110/in.2022.22.e43

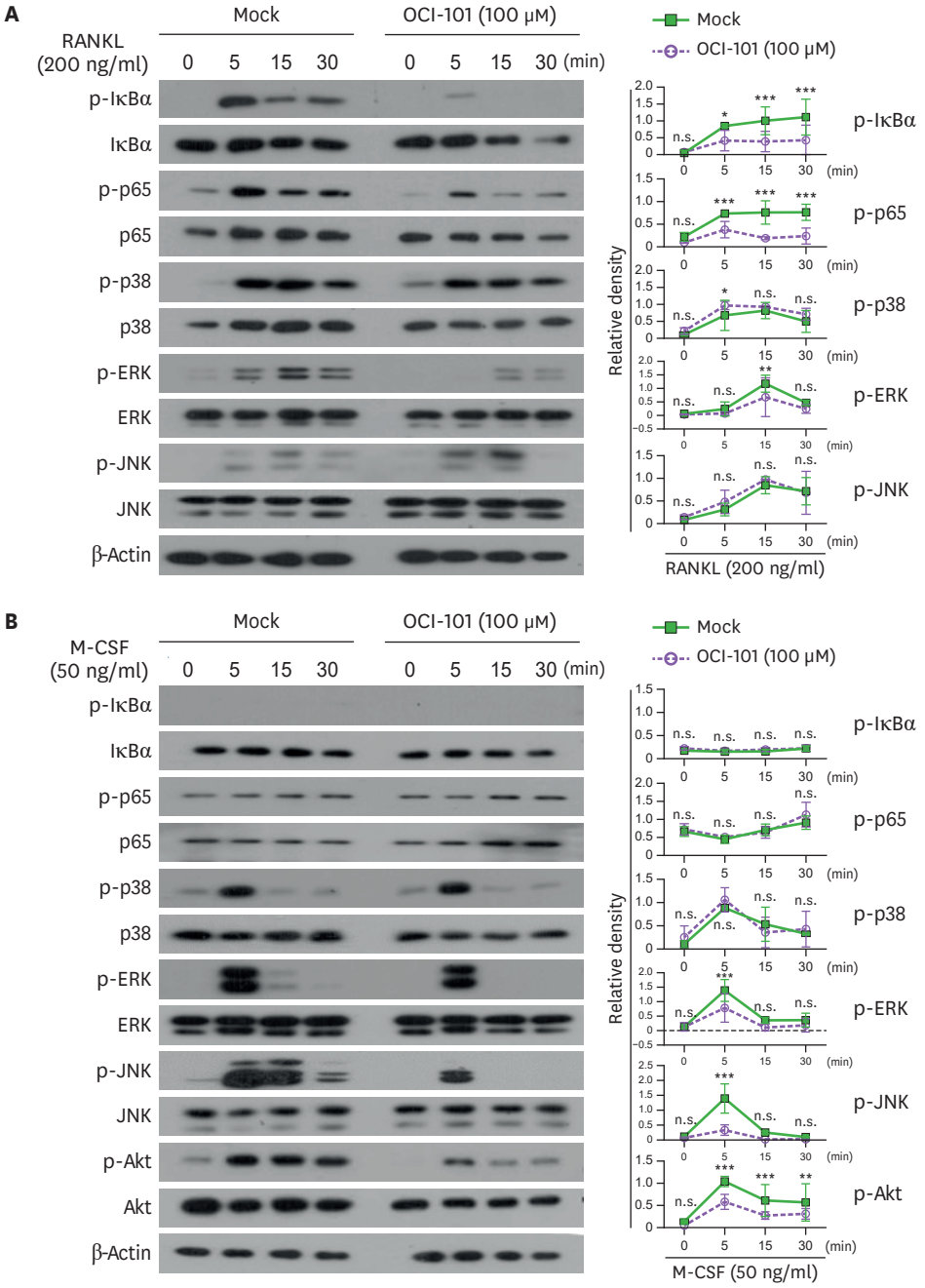

Figure 2. OCI-101 inhibits RANKL- and M-CSF-induced signaling. (A) The effect of OCI-101 on RANKL-induced signaling pathway. The cultured BMMs were preincubated with 100 μM OCI-101 for 12 h, and the cells were stimulated with RANKL (200 ng/ml) for the indicated times. The cells were then analyzed by immunoblotting with antibodies recognizing phosphorylated and total IκBα, p65, p38, ERK and JNK (left panel). β-Actin was used as the loading control. The relative level of phosphorylated proteins was calculated after normalization to total protein input (right panel). (B) The effect of OCI-101 on M-CSF-induced signaling pathway.
n.s., not significant.
*p<0.05; **p<0.01; ***p<0.001.

we observed that the extent of bone loss in the trabecular bones of the femur in OVX mice was not significantly altered by 1 mg/kg OCI-101 treatment, while OVX-induced bone loss in the trabecular bones was rescued by 10 mg/kg OCI-101 treatment (**Fig. 3A**). Consistent with the results, the number of $TRAP^+$ OCs in the trabecular region of femurs was decreased (26.9%

https://doi.org/10.4110/in.2022.22.e43

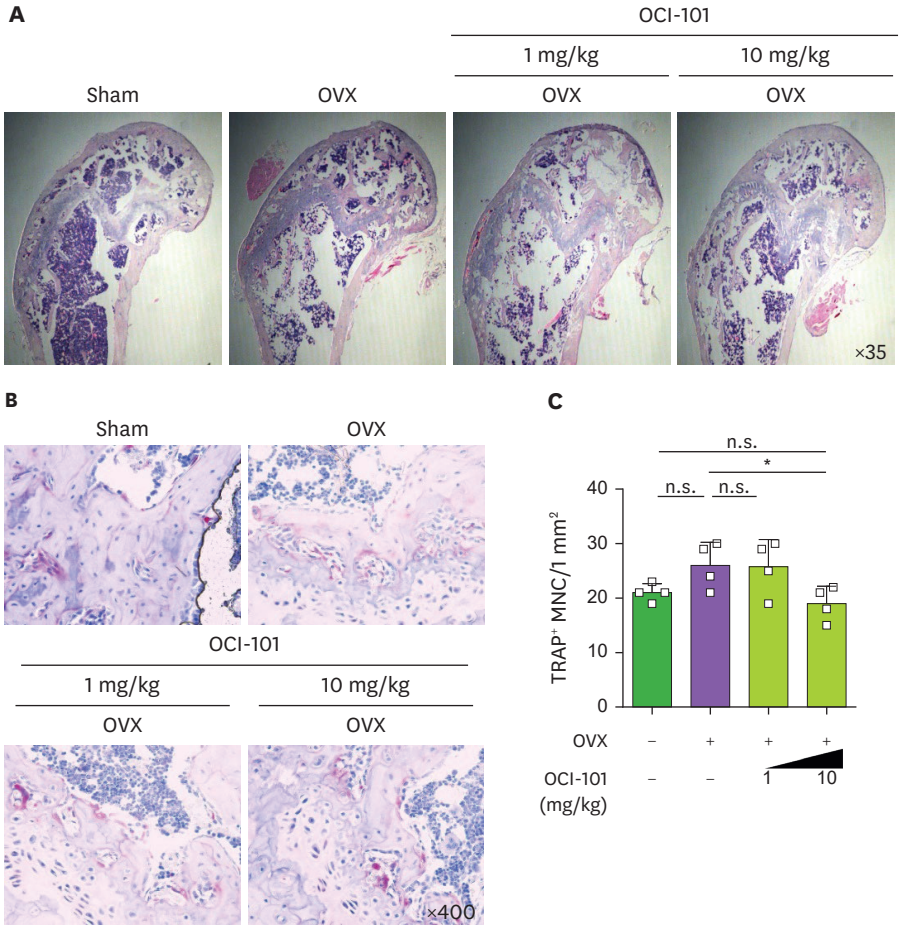

Figure 3. Morphological and histological analyses of trabecular bones in OCI-101-treated OVX mice. (A) Rescued phenotype of bone histological morphology by OCI-101 treatment in OVX mice. Femurs of mice (8-week-old, n=10–11/group) were fixed with 10% formalin, decalcified and embedded in paraffin. The paraffin sections were stained with TRAP and hematoxylin (original magnification, ×35). Sham, sham operation. OVX, ovariectomy. (B) The number of TRAP⁺ OCs in the distal femurs of OCI-101-treated OVX mice was decreased. Paraffin sections were stained with TRAP and hematoxylin (original magnification, ×200). (C) The number of TRAP⁺ OCs in the distal femur was counted.
n.s., not significant.
*p<0.05.

reduction, p<0.05) in OCI-101 (10 mg/kg)-treated OVX mice compared to that of OVX control mice (**Fig. 3B and C**). Hence, these results indicate that OCI-101 acts as an inhibitor in OVX-induced bone loss by reducing OC formation *in vivo*.

OCI-101 prevents OVX-induced bone loss in mice

We next analyzed bone microarchitecture changes in OCI-101-treated OVX mice by micro-CT. Bone parameters and 3-dimensional images of the trabecular region of the femurs were measured and quantified using micro-CT (**Fig. 4A**). Based on the imaging analysis, the extent of bone loss in the trabecular bones of the femur in OVX mice was not significantly altered by 1 mg/kg OCI-101 treatment (**Fig. 4A**). However, we observed that the increased bone loss of the trabecular bones in OVX mice was clearly inhibited by 10 mg/kg OCI-101 treatment (**Fig. 4A**). Consistent with the results, we observed the rescued phenotypes in the analysis of bone parameters after 10 mg/kg OCI-101 treatment (**Fig. 4B**). The BMD of the femurs was significantly increased (12.8% higher [p<0.001]) with high-dose OCI-101 treatment (10 mg/kg) in OVX mice compared to that in the femurs of OVX control mice (**Fig. 4B**, first panel). The trabecular bone volume fraction was 34.8% higher (p<0.01) in OVX mice treated with a

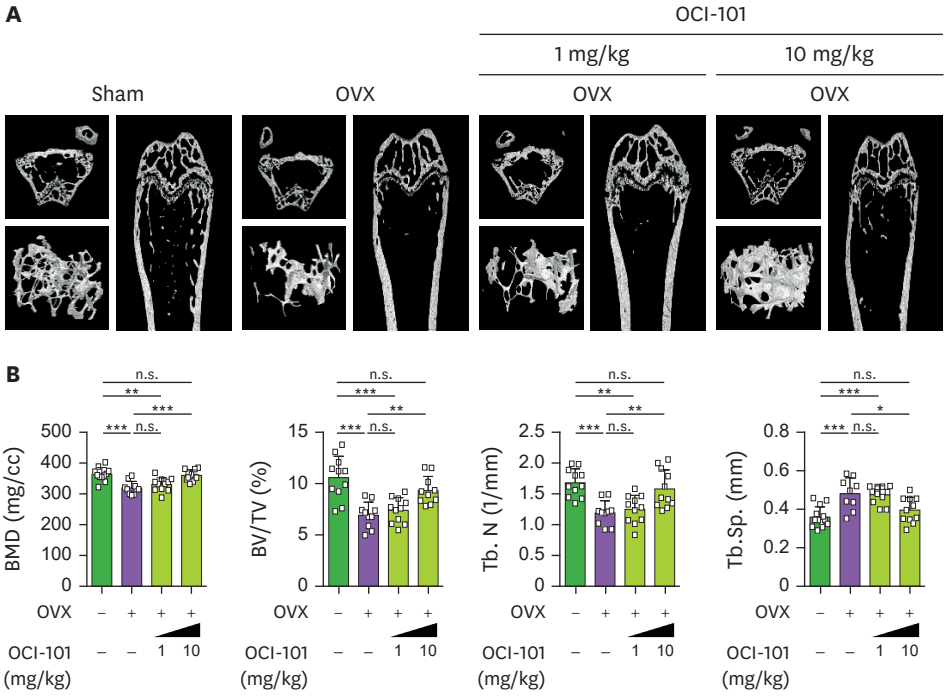

Figure 4. Micro-CT analyses of trabecular bones in OCI-101-treated OVX mice. (A) Three-dimensional microstructural analysis of the distal femur in OCI-101-treated OVX mice. Femurs of mice (8-week-old, n=10–11/group) were fixed with 10% formalin and analyzed by micro-CT. Micro-CT images of the femur are shown. (B) Three-dimensional trabecular structural parameters in distal femurs from OCI-101-treated OVX mice. The following parameters were analyzed: BMD, BV/TV, Tb. N and Tb.Sp.
n.s., not significant; BV/TV, trabecular bone volume fraction, Tb. N, trabecular number; Tb.Sp, trabecular spacing.
$^{*}p<0.05$; $^{**}p<0.01$; $^{***}p<0.001$.

high concentration (10 mg/kg) of OCI-101 than in OVX control mice (**Fig. 4B**, second panel). Furthermore, the Tb. N was 32.9% higher ($p<0.01$) in OCI-101 (10 mg/kg)-treated OVX mice than in OVX control mice, while trabecular spacing was 17.8% lower ($p<0.05$) in OCI-101 (10 mg/kg)-treated OVX mice than in OVX control mice (**Fig. 4B**, third and fourth panels). Taken together, these results suggest that OCI-101 has protective effects on the OVX-induced osteoporotic-like bone phenotype *in vivo*.

DISCUSSION

OCs are terminally differentiated and specialized multinucleated cells exclusively responsible for physiological and pathological bone destruction (2,3). Mature OCs are formed by cell fusion of $TRAP^{+}$ mononuclear OC precursors during osteoclastogenesis (2,3). Therefore, targeting osteoclastogenesis is considered a good therapeutic strategy for management of metabolic bone diseases, including postmenopausal osteoporosis and osteoarthritis, which are characterized by accelerated bone destruction by OCs. In our current study, we identified a novel inhibitor, OCI-101, targeting OC differentiation. Our findings reveal that 1) OCI-101 is an inhibitor of osteoclastogenesis, 2) OCI-101 inhibits multiple RANKL- and M-CSF-induced signaling, and 3) OCI-101 has protective effects against OVX-induced osteoporotic-like bone loss.

RANK-RANKL signaling is a critical osteoclastogenic pathway. The stimulation of RANK by RANKL recruits TRAFs, such as TRAF2, 5, and 6, to the cytoplasmic tail of trimeric RANK, thereby finally activating the transcription factors AP-1 and NF-κB (2,3). Among the TRAFs,

TRAF6 plays a pivotal role in the activation of downstream signaling cascades, including MAPK and NF-κB pathways during RANKL-induced osteoclastogenesis (30). RANKL-induced NF-κB activation can trigger the induction of RANKL target gene expression (31,32). Particularly NFATc1, a master regulator of osteoclastogenesis, is one of the key target genes of NF-κB in RANKL-induced osteoclastogenesis (33). Thus, NF-κB activation is crucial for RANKL-induced osteoclastogenesis. In our current study, we showed that OCI-101 inhibits RANKL-induced OC differentiation via downregulation of NF-κB pathways (**Figs. 1** and **2A**). The phosphorylation of IκBα and p65 in the NF-κB pathway was significantly reduced by OCI-101 treatment (**Fig. 2A**). The phosphorylation of IκBα by the IKK complex can lead to ubiquitin-mediated IκBα degradation, resulting in activation and nuclear translocation of NF-κB (34). The phosphorylation of p65 induces a conformational change that promotes its stability and interaction with cofactors of transcriptional machinery, thereby increasing NF-κB transcriptional activity (35,36). Thus, this process may explain that TRAF6-mediated IKK signaling pathways are inhibited by OCI-101 in RANKL-induced osteoclastogenesis.

The significance of RANKL-induced MAPK pathway activation is also well documented in osteoclastogenesis (2,3). In particular, the phosphorylation of p38, JNK and ERK in OC precursors by RANKL-induced TRAF6 signal transduction pathways is crucial for OC differentiation (37,38). The phosphorylation of p38 activates microphthalmia-associated transcription factors and NFATc1, which are responsible for the induction of osteoclastogenic genes, such as TRAP and cathepsin K (39,40). The phosphorylation of JNK is involved in the activation of the transcription factor c-Jun in RANKL-induced osteoclastogenesis (41,42). RANKL-induced ERK activation induces c-Fos phosphorylation and matrix metalloproteinase 9 expression (43,44). In our current study, we showed that the phosphorylation of ERK, but not that of p38 or JNK, by RANKL stimulation was reduced by OCI-101 treatment (**Fig. 2A**). Thus, it is possible that TRAF6 itself or the TRAF6 upstream signaling pathway is not the direct target of OCI-101. Hence, we presume that OCI-101 plays functionally distinct roles in blocking ERK activation of RANKL-RANK-TRAF6-mediated signaling pathways. RANKL-induced ERK activation is crucial for osteoclastogenesis (45,46). ERK1 deficiency reduces OC differentiation, activation and survival (47). Furthermore, it has been reported that M-CSF signaling is also linked to ERK activation in osteoclastogenesis (44). M-CSF-induced ERK activation leads to OC proliferation and survival (48,49). Collectively, ERK activation is mediated by both RANKL- and M-CSF-induced signaling in osteoclastogenesis. Based on our observations showing the reduction of ERK phosphorylation by OCI-101 (**Fig. 2**), we hypothesized that the inhibitory effects of OCI-101 might be linked to both RANKL- and M-CSF-induced ERK activation in osteoclastogenesis. However, a direct target of OCI-101 for the ERK signaling pathway was not identified in this study; thus, further studies are required to elucidate how OCI-101 modulates the RANKL-induced ERK activation pathway in osteoclastogenesis.

In conclusion, we show that OCI-101 is a novel inhibitor of osteoclastogenesis. OCI-101 inhibits OC differentiation by blocking multiple RANKL- and M-CSF-induced signaling pathways. Finally, we show that OCI-101 prevents OVX-induced osteoporotic-like bone loss by suppressing OC differentiation in mice. Hence, these results show that OCI-101 is a good drug candidate to treat postmenopausal osteoporosis and inflammatory bone-related diseases.

ACKNOWLEDGEMENTS

This research was supported by the Basic Science Research Program through the National Research Foundation of Korea (NRF) and was funded by the Ministry of Education (NRF-2019R1A2C1084311, 2019M3F6A1109486 and 2022R1A2C1004076).

REFERENCES

1. Amarasekara DS, Kim S, Rho J. Regulation of osteoblast differentiation by cytokine networks. *Int J Mol Sci* 2021;22:2851.
PUBMED | CROSSREF
2. Amarasekara DS, Yun H, Kim S, Lee N, Kim H, Rho J. Regulation of osteoclast differentiation by cytokine networks. *Immune Netw* 2018;18:e8.
PUBMED | CROSSREF
3. Walsh MC, Kim N, Kadono Y, Rho J, Lee SY, Lorenzo J, Choi Y. Osteoimmunology: interplay between the immune system and bone metabolism. *Annu Rev Immunol* 2006;24:33-63.
PUBMED | CROSSREF
4. Amarasekara DS, Yu J, Rho J. Bone loss triggered by the cytokine network in inflammatory autoimmune diseases. *J Immunol Res* 2015;2015:832127.
PUBMED | CROSSREF
5. Darnay BG, Besse A, Poblenz AT, Lamothe B, Jacoby JJ. TRAFs in RANK signaling. *Adv Exp Med Biol* 2007;597:152-159.
PUBMED | CROSSREF
6. Kim N, Takami M, Rho J, Josien R, Choi Y. A novel member of the leukocyte receptor complex regulates osteoclast differentiation. *J Exp Med* 2002;195:201-209.
PUBMED | CROSSREF
7. Lee SH, Rho J, Jeong D, Sul JY, Kim T, Kim N, Kang JS, Miyamoto T, Suda T, Lee SK, et al. v-ATPase V0 subunit d2-deficient mice exhibit impaired osteoclast fusion and increased bone formation. *Nat Med* 2006;12:1403-1409.
PUBMED | CROSSREF
8. Rho J, Altmann CR, Socci ND, Merkov L, Kim N, So H, Lee O, Takami M, Brivanlou AH, Choi Y. Gene expression profiling of osteoclast differentiation by combined suppression subtractive hybridization (SSH) and cDNA microarray analysis. *DNA Cell Biol* 2002;21:541-549.
PUBMED | CROSSREF
9. Ji MX, Yu Q. Primary osteoporosis in postmenopausal women. *Chronic Dis Transl Med* 2015;1:9-13.
PUBMED | CROSSREF
10. Riggs BL. The mechanisms of estrogen regulation of bone resorption. *J Clin Invest* 2000;106:1203-1204.
PUBMED | CROSSREF
11. Pfeilschifter J. Hormone replacement and selective estrogen receptor modulators (SERMS) in the prevention and treatment of postmenopausal osteoporosis. *Orthopade* 2001;30:462-472.
PUBMED | CROSSREF
12. Migliaccio S, Brama M, Spera G. The differential effects of bisphosphonates, SERMS (selective estrogen receptor modulators), and parathyroid hormone on bone remodeling in osteoporosis. *Clin Interv Aging* 2007;2:55-64.
PUBMED | CROSSREF
13. Anastasilakis AD, Polyzos SA, Makras P. Therapy of endocrine disease: denosumab vs bisphosphonates for the treatment of postmenopausal osteoporosis. *Eur J Endocrinol* 2018;179:R31-R45.
PUBMED | CROSSREF
14. Khosla S, Bilezikian JP, Dempster DW, Lewiecki EM, Miller PD, Neer RM, Recker RR, Shane E, Shoback D, Potts JT. Benefits and risks of bisphosphonate therapy for osteoporosis. *J Clin Endocrinol Metab* 2012;97:2272-2282.
PUBMED | CROSSREF
15. Liberman UA, Weiss SR, Bröll J, Minne HW, Quan H, Bell NH, Rodriguez-Portales J, Downs RW Jr, Dequeker J, Favus M, et al. Effect of oral alendronate on bone mineral density and the incidence of fractures in postmenopausal osteoporosis. *N Engl J Med* 1995;333:1437-1443.
PUBMED | CROSSREF

16. Ma S, Goh EL, Jin A, Bhattacharya R, Boughton OR, Patel B, Karunaratne A, Vo NT, Atwood R, Cobb JP, et al. Long-term effects of bisphosphonate therapy: perforations, microcracks and mechanical properties. *Sci Rep* 2017;7:43399.
PUBMED | CROSSREF

17. Zhang N, Zhang ZK, Yu Y, Zhuo Z, Zhang G, Zhang BT. Pros and cons of denosumab treatment for osteoporosis and implication for RANKL aptamer therapy. *Front Cell Dev Biol* 2020;8:325.
PUBMED | CROSSREF

18. Chandran T, Venkatachalam I. Efficacy and safety of denosumab compared to bisphosphonates in improving bone strength in postmenopausal osteoporosis: a systematic review. *Singapore Med J* 2019;60:364-378.
PUBMED | CROSSREF

19. Black DM, Schwartz AV, Ensrud KE, Cauley JA, Levis S, Quandt SA, Satterfield S, Wallace RB, Bauer DC, Palermo L, et al. Effects of continuing or stopping alendronate after 5 years of treatment: the Fracture Intervention Trial Long-term Extension (FLEX): a randomized trial. *JAMA* 2006;296:2927-2938.
PUBMED | CROSSREF

20. Bone HG, Wagman RB, Brandi ML, Brown JP, Chapurlat R, Cummings SR, Czerwiński E, Fahrleitner-Pammer A, Kendler DL, Lippuner K, et al. 10 years of denosumab treatment in postmenopausal women with osteoporosis: results from the phase 3 randomised FREEDOM trial and open-label extension. *Lancet Diabetes Endocrinol* 2017;5:513-523.
PUBMED | CROSSREF

21. Lorentzon M. Treating osteoporosis to prevent fractures: current concepts and future developments. *J Intern Med* 2019;285:381-394.
PUBMED | CROSSREF

22. Bone HG, Bolognese MA, Yuen CK, Kendler DL, Wang H, Liu Y, San Martin J. Effects of denosumab on bone mineral density and bone turnover in postmenopausal women. *J Clin Endocrinol Metab* 2008;93:2149-2157.
PUBMED | CROSSREF

23. Kim B, Cho YJ, Lim W. Osteoporosis therapies and their mechanisms of action (review). *Exp Ther Med* 2021;22:1379.
PUBMED | CROSSREF

24. Wu J, Zhang Q, Yan G, Jin X. Denosumab compared to bisphosphonates to treat postmenopausal osteoporosis: a meta-analysis. *J Orthop Surg* 2018;13:194.
PUBMED | CROSSREF

25. Shin B, Yu J, Park ES, Choi S, Yu J, Hwang JM, Yun H, Chung YH, Hong KS, Choi JS, et al. Secretion of a truncated osteopetrosis-associated transmembrane protein 1 (OSTM1) mutant inhibits osteoclastogenesis through down-regulation of the B lymphocyte-induced maturation protein 1 (BLIMP1)-nuclear factor of activated T cells c1 (NFATc1) axis. *J Biol Chem* 2014;289:35868-35881.
PUBMED | CROSSREF

26. Yu J, Yun H, Shin B, Kim Y, Park ES, Choi S, Yu J, Amarasekara DS, Kim S, Inoue J, et al. Interaction of tumor necrosis factor receptor-associated factor 6 (TRAF6) and Vav3 in the receptor activator of nuclear factor κB (RANK) signaling complex enhances osteoclastogenesis. *J Biol Chem* 2016;291:20643-20660.
PUBMED | CROSSREF

27. Ha H, Shim KS, An H, Kim T, Ma JY. Water extract of *Spatholobus suberectus* inhibits osteoclast differentiation and bone resorption. *BMC Complement Altern Med* 2013;13:112.
PUBMED | CROSSREF

28. Yu J, Kim S, Lee N, Jeon H, Lee J, Takami M, Rho J. Pax5 negatively regulates osteoclastogenesis through downregulation of Blimp1. *Int J Mol Sci* 2021;22:2097.
PUBMED | CROSSREF

29. Kim T, Ha H, Kim N, Park ES, Rho J, Kim EC, Lorenzo J, Choi Y, Lee SH. ATP6v0d2 deficiency increases bone mass, but does not influence ovariectomy-induced bone loss. *Biochem Biophys Res Commun* 2010;403:73-78.
PUBMED | CROSSREF

30. Yamamoto M, Gohda J, Akiyama T, Inoue JI. TNF receptor-associated factor 6 (TRAF6) plays crucial roles in multiple biological systems through polyubiquitination-mediated NF-κB activation. *Proc Jpn Acad Ser B Phys Biol Sci* 2021;97:145-160.
PUBMED | CROSSREF

31. Iotsova V, Caamaño J, Loy J, Yang Y, Lewin A, Bravo R. Osteopetrosis in mice lacking NF-κB1 and NF-κB2. *Nat Med* 1997;3:1285-1289.
PUBMED | CROSSREF

32. Xing L, Bushnell TP, Carlson L, Tai Z, Tondravi M, Siebenlist U, Young F, Boyce BF. NF-κB p50 and p52 expression is not required for RANK-expressing osteoclast progenitor formation but is essential for RANK- and cytokine-mediated osteoclastogenesis. *J Bone Miner Res* 2002;17:1200-1210.
PUBMED | CROSSREF

33. Negishi-Koga T, Takayanagi H. Ca^{2+}-NFATc1 signaling is an essential axis of osteoclast differentiation. *Immunol Rev* 2009;231:241-256.
PUBMED | CROSSREF

34. Liu T, Zhang L, Joo D, Sun SC. NF-κB signaling in inflammation. *Signal Transduct Target Ther* 2017;2:17023.
PUBMED | CROSSREF

35. Lawrence T, Bebien M, Liu GY, Nizet V, Karin M. IKKα limits macrophage NF-κB activation and contributes to the resolution of inflammation. *Nature* 2005;434:1138-1143.
PUBMED | CROSSREF

36. Zhong H, Voll RE, Ghosh S. Phosphorylation of NF-κB p65 by PKA stimulates transcriptional activity by promoting a novel bivalent interaction with the coactivator CBP/p300. *Mol Cell* 1998;1:661-671.
PUBMED | CROSSREF

37. Asagiri M, Takayanagi H. The molecular understanding of osteoclast differentiation. *Bone* 2007;40:251-264.
PUBMED | CROSSREF

38. Kim H, Choi HK, Shin JH, Kim KH, Huh JY, Lee SA, Ko CY, Kim HS, Shin HI, Lee HJ, et al. Selective inhibition of RANK blocks osteoclast maturation and function and prevents bone loss in mice. *J Clin Invest* 2009;119:813-825.
PUBMED | CROSSREF

39. Mansky KC, Sankar U, Han J, Ostrowski MC. Microphthalmia transcription factor is a target of the p38 MAPK pathway in response to receptor activator of NF-κB ligand signaling. *J Biol Chem* 2002;277:11077-11083.
PUBMED | CROSSREF

40. Matsumoto M, Sudo T, Saito T, Osada H, Tsujimoto M. Involvement of p38 mitogen-activated protein kinase signaling pathway in osteoclastogenesis mediated by receptor activator of NF-κB ligand (RANKL). *J Biol Chem* 2000;275:31155-31161.
PUBMED | CROSSREF

41. David JP, Sabapathy K, Hoffmann O, Idarraga MH, Wagner EF. JNK1 modulates osteoclastogenesis through both c-Jun phosphorylation-dependent and -independent mechanisms. *J Cell Sci* 2002;115:4317-4325.
PUBMED | CROSSREF

42. Lee K, Seo I, Choi MH, Jeong D. Roles of mitogen-activated protein kinases in osteoclast biology. *Int J Mol Sci* 2018;19:3004.
PUBMED | CROSSREF

43. Sundaram K, Nishimura R, Senn J, Youssef RF, London SD, Reddy SV. RANK ligand signaling modulates the matrix metalloproteinase-9 gene expression during osteoclast differentiation. *Exp Cell Res* 2007;313:168-178.
PUBMED | CROSSREF

44. Wagner EF, Matsuo K. Signalling in osteoclasts and the role of Fos/AP1 proteins. *Ann Rheum Dis* 2003;62 Suppl 2:ii83-ii85.
PUBMED | CROSSREF

45. Meissner JD, Freund R, Krone D, Umeda PK, Chang KC, Gros G, Scheibe RJ. Extracellular signal-regulated kinase 1/2-mediated phosphorylation of p300 enhances myosin heavy chain I/β gene expression via acetylation of nuclear factor of activated T cells c1. *Nucleic Acids Res* 2011;39:5907-5925.
PUBMED | CROSSREF

46. Nakamura H, Hirata A, Tsuji T, Yamamoto T. Role of osteoclast extracellular signal-regulated kinase (ERK) in cell survival and maintenance of cell polarity. *J Bone Miner Res* 2003;18:1198-1205.
PUBMED | CROSSREF

47. He Y, Staser K, Rhodes SD, Liu Y, Wu X, Park SJ, Yuan J, Yang X, Li X, Jiang L, et al. Erk1 positively regulates osteoclast differentiation and bone resorptive activity. *PLoS One* 2011;6:e24780.
PUBMED | CROSSREF

48. Bradley EW, Ruan MM, Vrable A, Oursler MJ. Pathway crosstalk between Ras/Raf and PI3K in promotion of M-CSF-induced MEK/ERK-mediated osteoclast survival. *J Cell Biochem* 2008;104:1439-1451.
PUBMED | CROSSREF

49. Ross FP. M-CSF, c-Fms, and signaling in osteoclasts and their precursors. *Ann N Y Acad Sci* 2006;1068:110-116.
PUBMED | CROSSREF